*J. Fluid Mech.* (1988), *vol.* 187, *pp.* 507–532
*Printed in Great Britain*



# The dynamics of towed flexible cylinders Part 1. Neutrally buoyant elements

By A. P. DOWLING

Department of Engineering, University of Cambridge, Trumpington Street, Cambridge CB2 1PZ, UK

(Received 20 March 1987)

The transverse vibrations of a thin, flexible cylinder under nominally constant towing conditions are investigated. The cylinder is neutrally buoyant, of radius $a_A$ with a free end and very small bending stiffness. As the cylinder is towed with velocity $U$, the tangential drag causes the tension in the cylinder to increase from zero at its free end to a maximum at the towing point. Transverse vibrations of the cylinder are opposed by a normal viscous drag force. Both the normal and tangential viscous forces can be described conveniently in terms of drag coefficients $C_N$ and $C_T$. The ratio $C_N/C_T$ has a crucial effect on the motion of the cylinder. The form of the transverse displacement is found to be greatly influenced by the existence of a critical point at which the effect of tension in the cylinder is cancelled by a fluid loading term. Matched asymptotic expansions are used to extend the solution across this critical point to apply the downstream boundary condition. Displacements well upstream of the critical point have a simple form, while nearer to the critical point the solution depends on whether the normal drag coefficient $C_N$ is greater or less than one-half $C_T$.

The typical acoustic streamer geometry considered is found to be stable to transverse displacements at all towing speeds. Forced perturbations of frequency $\omega$ are investigated. At low frequencies they propagate effectively along the cylinder with speed $U$. At higher frequencies they are attenuated.

The effect of a rope drogue of length $l_R$, radius $a_R$, is investigated. Provided $\omega l_R a_R/Ua_A$ is very small, the drogue has the same effect as a small increase in the length of the cylinder. However at higher frequencies and for small values of the ratio $C_N/C_T$ attaching a drogue may be disadvantageous because it reduces the attenuation of high-frequency disturbances as they propagate down the cylinder.

## 1. Introduction

Towed instrumentation packages in the form of long flexible cylinders are used extensively to detect and analyse acoustic signals in the ocean. A typical geometry is illustrated in figure 1. It consists of a heavier-than-water cable attached at one end to a ship and at the other to a neutrally buoyant slender cylinder containing a sonar array. This cylinder is sometimes referred to as an acoustic 'streamer' or 'array'. There may possibly be a rope at the downstream end of the cylinder acting as a drogue. If such an arrangement is to give good resolution of the acoustic signals it detects, the instantaneous shape of the acoustic streamer must be known. When the ship maintains a constant velocity, the cylinder is straight and horizontal. However, changes in the ship's path will make it deform. In these two papers we analyse linear departures from the ideal case due, for example, to changes in ship speed or heading.

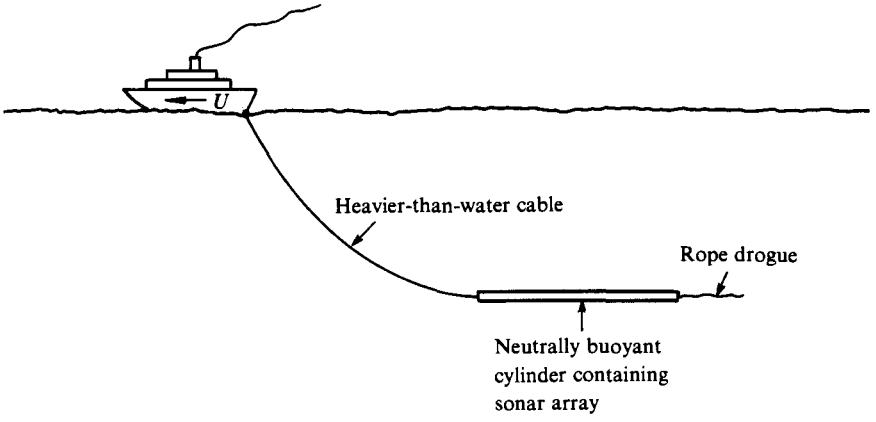


FIGURE 1. Typical geometry for a ship towing an array.

The aim of this work is to provide a simple means by which the shape of the towed system can be predicted either from the ship's path or from an accelerometer at the leading edge of the cylinder. Part 1 deals with the displacements of the neutrally buoyant elements, while Part 2 investigates the propagation of disturbances along the negatively buoyant cable. The results of Part 1 provide the downstream boundary conditions for the cable in Part 2.

Computer programs have been developed to calculate the three-dimensional path of a towed system as a ship manoeuvres (see for example Ivers & Mudie 1973, 1975; Huston & Kamman 1981; Sanders 1982; Ablow & Schechter 1983). In general these packages require considerable computing resources and, if they are to run in real time, certain simplifying assumptions must be made. Since we are investigating small departures from constant velocity, we adopt a different approach, and linearize the transverse equations of motion. Païdoussis (1966, 1968) derived a linearized form of the transverse momentum equation for neutrally buoyant flexible cylinders with an axial flow. A term has been omitted from these early versions and Païdoussis (1973) gives the correct form of the equation of motion. Disturbances of frequency $\omega$ satisfy a linear fourth-order differential equation. The coefficient of the fourth derivative depends on the bending stiffness of the cylinder. Perturbations of cylinders whose response depends on their bending stiffness have been extensively studied in the literature (see for example Hawthorne 1961; Païdoussis 1966, 1968, 1973; Lee 1978; Prokhorovich, Prokhorovich & Smirnov 1982).

However, acoustic streamers are very long in comparison with their radius $a_A$, and, for motions with wavelengths comparable with the cylinder length, the restoring force due to bending stiffness is exceedingly small. It is therefore appropriate to recognize this and neglect the effect of the bending stiffness over most of the cylinder. This approximation has been made by Ortloff & Ives (1969), Kennedy (1980), Kennedy & Strahan (1981) and Lee & Kennedy (1985). The differential equation then reduces to second order, the coefficient of the highest derivative being $T(x)-\rho_0 \pi a_A^2 U^2$, where $T(x)$ is the tension in the cylinder and varies along its length. $U$ is the mean flow velocity and $\rho_0$ the density of the surrounding fluid; $\rho_0 \pi a_A^2 U^2$ arises due to the effect of fluid loading.

In §2–4 we consider a thin, neutrally buoyant, flexible cylinder with its downstream end unrestrained. $T(x)$ then vanishes at this free end, and increases along the cylinder due to tangential drag. It is well known that the transverse

displacements of a tensioned string *in vacuo* satisfy a hyperbolic differential equation. When fluid loading is included, the equation remains hyperbolic over most of its length, but is elliptic near the free end, having a regular singular point at $x_c$, a critical position at which $T(x_c) = \rho_0 \pi a_A^2 U^2$. Ortloff & Ives and Kennedy & Strahan base their work on Païdoussis' early erroneous equation of motion, and find one of the solutions of their linear, second-order equation to be unbounded at $x_c$. They therefore reject this solution and the downstream boundary condition and describe the response of the cylinder in terms of the other (finite) solution. However, when the correct form of Païdoussis' equation is used, and for reasonable values of the drag coefficients, both solutions are finite at the critical position, although one solution has a branch point there. Hence, before the downstream boundary condition can be applied, further investigation is needed to see how this solution behaves as $x$ crosses $x_c$. In the region of $x_c$ the response is controlled by the bending stiffness of the cylinder. We therefore use the fourth-order equation in the region of $x_c$, and the method of matched asymptotic expansions to join these 'inner' bending solutions to the 'outer' tension-dominated response. In this way, the general solution for the vibration of a fluid-loaded cylinder, in the limit of small bending stiffness, can be found. Application of the free-end boundary condition then leads to an analytical expression for transverse displacements of the towed cylinder at frequency $\omega$. The displacements are found to have a simple form well upstream of $x_c$. Nearer to $x_c$ the expression is more complicated and depends on whether the normal drag coefficient $C_N$ is greater or less than half the tangential drag coefficient $C_T$.

In §3 we investigate the stability of a neutrally buoyant towed cylinder by seeing whether there are any free modes that grow in time. A practical streamer geometry is found to be stable at all towing speeds.

Since the towed cylinder is stable, it is appropriate to determine its response to forcing at its upstream end. At low frequencies for which $\omega l_A/U$ is small the disturbances propagate along the cylinder, virtually unchanged in amplitude and with a phase speed $U$, while for higher frequencies the disturbances decay in amplitude along the streamer. The first form of motion is often described as 'worm-in-a-hole' because all points of the cylinder take the same track. This motion is compatible with observations of low-frequency oscillations of towed arrays.

So far we have assumed the end of the cylinder to be free. However in many practical situations it is attached to a rope drogue. In §5 we investigate the effect of a rope drogue. We use the work in the earlier sections to describe the transverse motions of the rope which has a free end, and apply continuity of displacement and force at the junction of the drogue and cylinder. If $\omega l_R a_R/U a_A$ is very small, the main effect of the drogue is found to be the same as an increase in length of the cylinder by an amount $l_R a_R/a_A$, where $a_R$ and $l_R$ are the radius and length of the rope drogue respectively. At higher frequencies a drogue can have an adverse effect if the ratio $C_N/C_T$ is small. Then attaching a drogue reduces the attenuation of high-frequency transverse disturbances as they propagate down the cylinder.

## 2. The transverse motion of a neutrally buoyant flexible cylinder

Consider an acoustic streamer consisting of a long flexible cylinder of length $l_A$, radius $a_A$, towed in the negative $x$-direction at a constant speed $U$. If the cylinder is neutrally buoyant its mean position is horizontal. We will investigate linear departures from this arrangement and choose a frame of reference in which the distant fluid has a velocity $(U, 0, 0)$, with the origin at the mean position of the

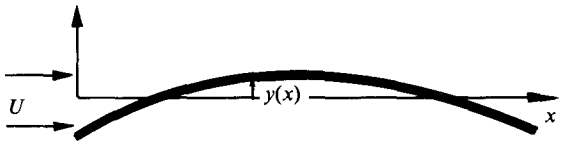


FIGURE 2. Linear perturbations of the towed cylinder, viewed in a frame of reference in which the distant fluid has velocity $(U, 0, 0)$.

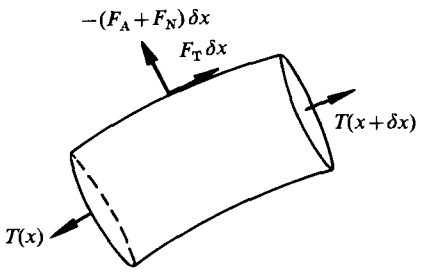


FIGURE 3. Forces acting on a small length, $\delta x$, of the neutrally buoyant cylinder.

upstream end of the cylinder as shown in figure 2. It follows from the neutral buoyancy of the cylinder, and the linearity of the disturbances, that perturbations in the $(y = 0)$- and $(z = 0)$-planes satisfy identical uncoupled equations. It is therefore sufficient just to investigate the motion in one plane, $(z = 0)$ say.

The equation of motion of the cylinder may be derived by considering the balance of forces on a small length as shown in figure 3. Let $T(x)$ be the variable tension in the cylinder, $F_N$ and $F_T$ the viscous forces acting on the cylinder per unit length in the local normal and tangential directions respectively, and $F_A$ the inviscid force due to the acceleration of the virtual mass of the cylinder. Resolving in the $x$-direction gives, to zeroth order in the perturbations,

$$F_T + \frac{\partial T}{\partial x} = 0. \tag{2.1}$$

The transverse momentum balance gives, to first order in the disturbances,

$$m\frac{\partial^2 y}{\partial t^2} = \frac{\partial}{\partial x}\left(T\frac{\partial y}{\partial x}\right) - F_A - F_N + F_T\frac{\partial y}{\partial x} - B\frac{\partial^4 y}{\partial x^4}, \tag{2.2}$$

where $m$ is the mass of the cylinder per unit length and $B$ is its bending stiffness. This is Païdoussis' equation. The term $F_T\,\partial y/\partial x$ was omitted in Païdoussis' early work (see for example Païdoussis 1966, 1968). This error was later corrected (Païdoussis 1973 and Païdoussis & Yu 1976) but unfortunately the earlier erroneous form has been adopted in much of the towed-array literature (Ortloff & Ives 1969; Kennedy 1980; Kennedy & Strahan 1981). As Païdoussis (1973) points out, omitting the term $F_T\,\partial y/\partial x$ is equivalent to taking the tangential viscous force to act in the $x$-direction rather than in the instantaneous tangential direction.

$F_A$ is the force required to accelerate the neighbouring fluid as the cylinder deforms. Provided the flow does not separate, the expression derived by Lighthill (1960) may be used:

$$F_A = \rho_0 \pi a_A^2 \left(\frac{\partial}{\partial t} + U\frac{\partial}{\partial x}\right)^2 y, \tag{2.3}$$

where $\rho_0$ is the fluid density.

The viscous forces acting on a long, thin flexible cylinder are discussed by Taylor (1952). He proposes the form

$$F_N = \tfrac{1}{2}\rho_0 V^2\{2a_A C_D \sin^2 i + 2\pi a_A C_N \sin i\}, \tag{2.4a}$$

$$F_T = \rho_0 V^2 \pi a_A C_T \cos i, \tag{2.4b}$$

where $V$ is the magnitude of the relative velocity between the cylinder and the distant flow, and $i$ is the angle between this relative velocity and the local tangent. For linear perturbations of a neutrally buoyant element, $V$ is equal to $U$ and $i$ is small,

$$\sin i \approx i \approx \frac{1}{U}\frac{\partial y}{\partial t} + \frac{\partial y}{\partial x}, \quad \cos i \approx 1.$$

These expressions therefore reduce to

$$F_N = \rho_0 \pi a_A U C_N \left(\frac{\partial y}{\partial t} + U\frac{\partial y}{\partial x}\right), \tag{2.5a}$$

$$F_T = \rho_0 \pi a_A U^2 C_T. \tag{2.5b}$$

With this form for the tangential drag the longitudinal momentum equation (2.1) may be integrated immediately to give

$$T(x) = T(l_A) + \rho_0 \pi a_A U^2 C_T (l_A - x), \tag{2.6}$$

$T(l_A)$ is the tension at the downstream end of the array, and vanishes if the end is free. Then $T(0)$, the tension at the upstream end, is directly proportional to the drag coefficient $C_T$. Hence $C_T$ may be inferred from measurements of $T(0)$. Data from large-scale experiments suggest $C_T = 0.0025$ (Andrew private communication 1984). Ni & Hansen (1978) obtained similar values of $C_T$ for a range of Reynolds numbers in their rig experiments. There is less evidence about the appropriate value of $C_N$. Taylor discusses in some detail how the value of $C_N$ would vary in the range $0 \leqslant C_N \leqslant C_T$ depending on the type of roughness on the cylinder. We will therefore investigate the effect of varying $C_N$ within this range.

When the expressions for $F_A$ and $F_N$ in (2.3) and (2.5) are substituted into the transverse momentum equation (2.2) they lead to

$$\rho_0 \pi a_A^2 \frac{\partial^2 y}{\partial t^2} = (T(x) - \rho_0 \pi a_A^2 U^2)\frac{\partial^2 y}{\partial x^2} - \rho_0 \pi a_A^2 \left(\frac{\partial^2 y}{\partial t^2} + 2U\frac{\partial^2 y}{\partial x\,\partial t}\right)$$

$$- \rho_0 \pi a_A U C_N \left(\frac{\partial y}{\partial t} + U\frac{\partial y}{\partial x}\right) - B\frac{\partial^4 y}{\partial x^4}. \tag{2.7}$$

The coefficient of the second derivative of $y$ vanishes at a position $x_c$, where $T(x_c)$ is equal to the fluid-loading term $\rho_0 \pi a_A^2 U^2$. Using (2.6) to rewrite $T(x)$ shows that

$$T(x) - \rho_0 \pi a_A^2 U^2 = \rho_0 \pi a_A U^2 C_T (x_c - x), \tag{2.8}$$

where

$$x_c = l_A + \frac{T(l_A)}{\rho_0 \pi a_A U^2 C_T} - \frac{a_A}{C_T}. \tag{2.9}$$

$x_c$ lies on the cylinder if

$$l_A \geqslant x_c \geqslant 0,$$

i.e. if

$$1 \geqslant \frac{T(l_A)}{\rho_0 \pi a_A^2 U^2} \geqslant 1 - \frac{l_A C_T}{a_A}. \tag{2.10}$$

Since we are considering linear disturbances we may investigate each Fourier component separately. For modes with time dependence $e^{i\omega t}$, equation (2.7) reduces to

$$\frac{B}{\rho_0 \pi a_A U^2 C_T}\frac{\partial^4 y}{\partial x^4}-(x_c-x)\frac{\partial^2 y}{\partial x^2}+\left(\frac{2i\omega a_A}{UC_T}+\frac{C_N}{C_T}\right)\frac{\partial y}{\partial x}+\frac{i\omega}{U}\left(\frac{2i\omega a_A}{UC_T}+\frac{C_N}{C_T}\right)y=0. \quad (2.11)$$

This may be cast into non-dimensional form by scaling lengths on $L$ (typically of order $l_A$). When a new variable $X = x/L$ is introduced, and with $y(x,t) = \mathrm{Re}\,(Y(X)\,e^{i\omega t})$, the transverse momentum equation becomes

$$\epsilon^3\frac{d^4Y}{dX^4}-(X_c-X)\frac{d^2Y}{dX^2}+b\frac{dY}{dX}+i\Omega bY=0, \quad (2.12)$$

$\epsilon = (B/L^3\rho_0\pi a_A U^2 C_T)^{\frac{1}{3}}$, is a small parameter because bending forces in the cylinder are very much less than the tension forces.

$$b=\frac{2i\Omega a_A}{LC_T}+\frac{C_N}{C_T}, \quad (2.13)$$

$\Omega$ is the non-dimensional frequency, $\omega L/U$, and $X_c$ is the non-dimensional critical position, $x_c/L$.

Away from regions with intense gradients the contribution from the fourth-order derivative in (2.12) is negligible because $\epsilon$ is small, and the equation reduces to

$$(X_c-X)\frac{d^2Y}{dX^2}-b\frac{dY}{dX}-i\Omega bY=0, \quad (2.14)$$

a second-order ordinary differential equation with a regular singular point at $X = X_c$. This only differs from the equation investigated by Ortloff & Ives (1969) and Kennedy & Strahan (1981) (derived from Païdoussis' erroneous version) in that in their equation the coefficient of the first derivative is, in this notation, $-1-b$ rather than $-b$. We will see later that this apparently small difference has considerable consequences.

The occurrence of a singularity at $X_c$ is not an artefact of the linearization. Ablow & Schechter (1983) investigate finite-difference solutions of general cylinder motion. They find that the matrix to be inverted is singular at the end of the cylinder where the tension vanishes. Since they have omitted a virtual mass term, which is the generalization of our linearized expression $\rho_0\pi a_A^2 U^2\partial^2 y/\partial x^2$ to arbitrary motion, their singularity is entirely equivalent to our singularity at $X_c$. Ablow & Schechter get around this difficulty in an *ad hoc* way by applying the downstream boundary condition at a point $P$, a short distance from the free end, and assuming the cylinder to be straight between $P$ and the free end. However for the linear disturbances considered here the effect of the singularity on the form of the solution can be investigated analytically.

Two solutions of (2.14) may be obtained by the standard method (Ince 1956) of trying a series solution of the form

$$Y(X) = (X_c-X)^\sigma \sum_{n=0}^{\infty} a_n (X_c-X)^n.$$

The indicial equation shows $\sigma$ to be equal either to 0 or to $1-b$. The general solution of (2.14) is then found to be

$$Y(X) = P\sum_{n=0}^{\infty}\frac{(\mathrm{i}\Omega b(X_c-X))^n}{n!(n+b-1)!}+Q(X_c-X)^{1-b}\sum_{n=0}^{\infty}\frac{(\mathrm{i}\Omega b(X_c-X))^n}{n!(n+1-b)!}, \tag{2.15}$$

$P$ and $Q$ are arbitrary constants. $Y(X)$ is a linear combination of two independent series solutions. The first solution is analytic while the second has a branch point at $X_c$. Both series converge for all $X$. Equation (2.13) shows that

$$1-b = 1-\frac{C_N}{C_T}-\frac{2\mathrm{i}\Omega a_A}{LC_T},$$

and so for $0 < C_N < C_T$ both solutions are finite at the critical position $X_C$.

In a typical problem, boundary conditions for the transverse motion are given at the two ends of the cylinder $X = 0$ and $X = l_A/L$. If the inequalities expressed in (2.10) are satisfied these two points are on either side of the critical position $X_c$. Let us now for definiteness consider a cylinder with a free downstream end at which $T(l_A)$ vanishes. Then the first inequality in (2.10) is automatically satisfied. Practical acoustic streamers are sufficiently long to ensure that $C_T l_A > a_A$, hence also meeting the second inequality. The critical point $X_c$ therefore lies somewhere between the two ends where the boundary conditions are specified. Before these boundary conditions can be applied, we need to determine how the solution expressed in (2.15) varies as $X$ passes through $X_c$. There is no difficulty with the first series solution because it is continuous at $X_c$, but the second has a branch point there and the relevant cut must be found. Since the second series solution has large gradients in the vicinity of $X_c$, bending forces become important and the full fourth-order equation (2.12) is needed to determine the form of the deflections. The method of matched asymptotic expansions may be used to match these 'inner' bending solutions to the 'outer' tension-dominated disturbances described in (2.15).

It is worth noting that Ortloff & Ives (1969) and Kennedy & Strahan (1981) did not have these difficulties. The second independent solution to their equation is infinite at the critical point. They therefore reject it and the downstream boundary condition, and use the other bounded solution to describe motion in $X < X_c$. But we have seen that when the correct form of Païdoussis' equation is used, both independent solutions are finite at $X_c$ for reasonable values of the normal drag coefficient. The behaviour of the solutions as $X$ varies across $X_c$ must therefore be investigated in detail so that the downstream boundary condition may be applied.

The solutions of (2.12) are to be determined for small values of $\epsilon$ and $0 < \mathrm{Re}\,(b)$. Let us shift the origin by introducing a new variable $r = X_c - X$. Then with $Y(X) = \phi(r, \epsilon)$, $\phi$ satisfies

$$\epsilon^3\frac{\mathrm{d}^4\phi}{\mathrm{d}r^4}-r\frac{\mathrm{d}^2\phi}{\mathrm{d}r^2}-b\frac{\mathrm{d}\phi}{\mathrm{d}r}+\mathrm{i}\Omega b\phi = 0. \tag{2.16}$$

For small $\epsilon$, it is appropriate to seek a series solution in powers of the small parameter $\epsilon^3$ which appears in (2.16);

$$\phi(r,\epsilon) = \phi_0(r)+\epsilon^3\phi_3(r)+\ldots.$$

The equation for $\phi_0(r)$ is

$$r\frac{\mathrm{d}^2\phi_0}{\mathrm{d}r_0^2}+b\frac{\mathrm{d}\phi_0}{\mathrm{d}r}-\mathrm{i}\Omega b\phi_0 = 0. \tag{2.17}$$

The general solution of this second-order equation has been given in (2.15) and is

$$\phi_0(r) = P \sum_{n=0}^{\infty} \frac{(\mathrm{i}\Omega br)^n}{n!\,(n+b-1)!} + Qr^{1-b} \sum_{n=0}^{\infty} \frac{(\mathrm{i}\Omega br)^n}{n!\,(n+1-b)!}. \tag{2.18}$$

Gradients of $\phi_0(r)$ become large near $r = 0$. Away from this region $\phi_0(r)$ describes deflections of the towed cylinder in which the response is determined by its mass, tension and fluid loading.

In the region of $r = 0$, the surface response is controlled by bending stiffness, and $\phi(r, \epsilon)$ varies rapidly. For this region then let us stretch the spatial coordinate and introduce $R \equiv r/\epsilon$ with $\phi(r, \epsilon) \equiv \Phi(R, \epsilon)$. An inner expansion for the displacements can be obtained by expanding $\Phi$ in ascending powers of $\epsilon$

$$\Phi(R, \epsilon) = \Phi_0(R) + \epsilon\Phi_1(R) + \ldots$$

$\Phi_0$ satisfies

$$\frac{\mathrm{d}^4\Phi_0}{\mathrm{d}R^4} - R\frac{\mathrm{d}^2\Phi_0}{\mathrm{d}R^2} - b\frac{\mathrm{d}\Phi_0}{\mathrm{d}R} = 0. \tag{2.19}$$

The four independent solutions of this linear fourth-order equation are determined in integral form in the Appendix where, in particular, their asymptotic forms for large $|R|$ are evaluated. It is found that for large positive $R$

$$\Phi_0(R) \approx A\pi^{\frac{1}{2}} R^{\frac{1}{2}b-\frac{5}{4}} \exp\left[\tfrac{2}{3}R^{\frac{3}{2}}\right] - (B\,\mathrm{e}^{\frac{1}{3}\mathrm{i}\pi b} + C\,\mathrm{e}^{-\frac{1}{3}\mathrm{i}\pi b})\,R^{1-b}(b-2)! + D, \tag{2.20}$$

$A$, $B$, $C$ and $D$ are arbitrary constants multiplying the four independent solutions and are to be determined by matching to the outer solution. When this inner solution is rewritten in terms of the outer variable $r$ it becomes

$$\Phi_0(r/\epsilon) \approx A\pi^{\frac{1}{2}} \left(\frac{r}{\epsilon}\right)^{\frac{1}{2}b-\frac{5}{4}} \exp\left[\frac{2}{3}\frac{r^{\frac{3}{2}}}{\epsilon^{\frac{3}{2}}}\right] - (B\,\mathrm{e}^{\frac{1}{3}\mathrm{i}\pi b} + C\,\mathrm{e}^{-\frac{1}{3}\mathrm{i}\pi b})\left(\frac{r}{\epsilon}\right)^{1-b} (b-2)! + D. \tag{2.21}$$

Matching this to the outer solution in (2.18) gives

$$A = 0, \quad Q = -(B\,\mathrm{e}^{\frac{1}{3}\mathrm{i}\pi b} + C\,\mathrm{e}^{-\frac{1}{3}\mathrm{i}\pi b})\,(1-b)!\,(b-2)!\,\epsilon^{b-1}, \quad P = D(b-1)! \tag{2.22}$$

Hence for $r \gg \epsilon$ we have

$$\phi_0(r) = P \sum_{n=0}^{\infty} \frac{(\mathrm{i}\Omega br)^n}{n!\,(n+b-1)!} + (Q_2 + Q_3)\,r^{1-b} \sum_{n=0}^{\infty} \frac{(\mathrm{i}\Omega br)^n}{n!\,(n+1-b)!} \tag{2.23}$$

with $Q_2 = -B\,\mathrm{e}^{\frac{1}{3}\mathrm{i}\pi b}\,(1-b)!\,(b-2)!\,\epsilon^{b-1}$ and $Q_3 = -C\,\mathrm{e}^{-\frac{1}{3}\mathrm{i}\pi b}\,(1-b)!\,(b-2)!\,\epsilon^{b-1}$.

When $r/\epsilon$ is large and negative with $1 \gg |r| \gg \epsilon$, the asymptotic form for $\Phi_0(R)$ evaluated in the Appendix (see equation (A 26)) shows that

$$\phi_0(r) \approx P \sum_{n=0}^{\infty} \frac{(\mathrm{i}\Omega br)^n}{n!\,(n+b-1)!} - \frac{(-r)^{1-b}}{(1-b)!}(Q_2\,\mathrm{e}^{-\mathrm{i}\pi b} + Q_3\,\mathrm{e}^{\mathrm{i}\pi b}) + \frac{\pi^{\frac{1}{2}}(-r)^{\frac{1}{2}b-\frac{5}{4}}\epsilon^{\frac{9}{4}-\frac{3}{2}b}}{(1-b)!\,(b-2)!}(Q_2\,\mathrm{e}^{-\mathrm{i}\theta} + Q_3\,\mathrm{e}^{\mathrm{i}\theta}), \tag{2.24}$$

for $-\epsilon \gg r \gg -1$, with $\theta = \pi\left(\frac{1}{2}b - \frac{3}{4}\right) + \frac{2}{3}(-r/\epsilon)^{\frac{3}{2}}$.

The first term on the right-hand side of (2.24) is just the series solution, describing the balance between tension and inertial forces, that is valid everywhere. The second and third terms describe motions downstream of the critical position with large gradients whose form is influenced by the bending stiffness of the cylinder.

Returning to the spatial variable $X$

$$Y(X) = P\sum_{n=0}^{\infty}\frac{(\mathrm{i}\Omega b(X_c-X))^n}{n!\,(n+b-1)!} + (Q_2+Q_3)(X_c-X)^{1-b}\sum_{n=0}^{\infty}\frac{(\mathrm{i}\Omega b(X_c-X))^n}{n!\,(n+1-b)} \quad \text{for } X_c-X \gg \epsilon, \quad (2.25a)$$

and

$$Y(X) \approx P\sum_{n=0}^{\infty}\frac{(\mathrm{i}\Omega b(X_c-X))^n}{n!\,(n+b-1)!} - \frac{(X-X_c)^{1-b}}{(1-b)!}(Q_2\,\mathrm{e}^{-\mathrm{i}\pi b}+Q_3\,\mathrm{e}^{\mathrm{i}\pi b}) + \pi^{\frac{1}{2}}\frac{(X-X_c)^{\frac{1}{2}b-\frac{5}{4}}\epsilon^{\frac{9}{4}-\frac{3}{2}b}}{(1-b)!\,(b-2)!}(Q_2\,\mathrm{e}^{-\mathrm{i}\theta}+Q_3\,\mathrm{e}^{\mathrm{i}\theta}) \quad \text{for } 1 \gg X-X_c \gg \epsilon, \quad (2.25b)$$

with $$\theta = \pi(\tfrac{1}{2}b-\tfrac{3}{4})+\tfrac{2}{3}((X-X_c)/\epsilon)^{\frac{3}{2}}.$$

To summarize then, perturbations of the cylinder upstream of the critical point are described by two linearly independent series solutions. The displacement typically varies over a non-dimensional lengthscale of order unity and the bending stiffness of the cylinder, characterized by the small non-dimensional parameter $\epsilon$, is unimportant in this range. The first series solution is always slowly varying and so is valid for all $X$. The second has a branch cut at the critical position, $X_c$, and large gradients near it. This second solution is extended across $X = X_c$ in the Appendix by using the full equation of cylinder motion including bending stiffness and is displayed in (2.25*b*). Not only is the appropriate branch cut determined by equation (2.25*b*), but it also shows the solution downstream of $X_c$ to contain wavelike disturbances with wavelengths of the order of $\epsilon$. Bending stiffness therefore has an important influence on the cylinder motion throughout this region. If either $Q_2$ or $Q_3$ is non-zero, the displacements of the cylinder vary over a long lengthscale well upstream of $X_c$, but have very small wavelengths throughout the tail region downstream of $X_c$. The coefficients $P$, $Q_2$ and $Q_3$ may be determined from the boundary conditions at the two ends of the array, $X = 0$ and $X = L_A = l_A/L$.

The two boundary conditions appropriate for a free end of a flexible cylinder have been derived by Hawthorne (1961). One condition is that there be no bending moment;

$$\frac{\mathrm{d}^2Y}{\mathrm{d}X^2} = 0 \quad \text{at } X = L_A. \quad (2.26)$$

The second condition arises from the transverse momentum balance for the tapered portion of the cylinder at its end. If this portion is very short its momentum is negligible, and the forces acting on it must cancel. The only significant forces on a short end at which the tension vanishes are due to bending resistance and the virtual mass of the fluid near the end. This has been evaluated by Hawthorne (1961) and Païdoussis (1966) and takes the form

$$B\frac{\partial^3 y}{\partial x^3}+f\rho_0\pi a_A^2 U\left(\frac{\partial y}{\partial t}+U\frac{\partial y}{\partial x}\right) = 0. \quad (2.27)$$

where $f$ is a non-dimensional parameter less than unity introduced to account for departures of the flow from two-dimensionality. In view of the uncertainty in the value of $f$, it is reassuring that our results will be found not to depend on the details of this boundary condition. For motions with time dependence $\mathrm{e}^{\mathrm{i}\omega t}$ (2.27) becomes

$$\epsilon^3\frac{\mathrm{d}^3Y}{\mathrm{d}X^3}+\frac{fa_A}{LC_T}\left(\frac{\mathrm{d}Y}{\mathrm{d}X}+\mathrm{i}\Omega Y\right) = 0. \quad (2.28)$$

We now substitute for $Y(X)$ from equation (2.25$b$) into the two boundary conditions (2.26) and (2.28). In the limit of small bending stiffness, this gives

$$Q_2\left[\frac{fE^{1-b}}{(-b)!}(e^{i\theta_E-i\pi b}-e^{-i\theta_E+i\pi b})-\frac{2i(1-f)\,\pi^{\frac{1}{2}}E^{\frac{1}{2}b+\frac{1}{4}}\epsilon^{\frac{3}{4}-\frac{3}{2}b}}{(b-2)!\,(1-b)!}\right]=P\frac{fb\Omega^2E^2\,e^{i\theta_E}}{(b+1)!}, \tag{2.29}$$

and

$$Q_3=-Q_2\,e^{-i2\theta_E}, \tag{2.30}$$

$E$ is the distance between the critical point and the free end. It is apparent from (2.9) that

$$E=L_A-X_c=a_A/LC_T. \tag{2.31}$$

In deriving (2.29) the product $\Omega E$ has been assumed to be small in comparison with unity. Acoustic streamers are sufficiently long in comparison with their radius for this to be a good approximation at the low frequencies of interest here. $\theta_E$ is defined by

$$\theta_E=\pi(\tfrac{1}{2}b-\tfrac{3}{4})+\tfrac{2}{3}(E/\epsilon)^{\frac{3}{2}}. \tag{2.32}$$

The solution of (2.29) and (2.30) has quite a different form according to whether $\mathrm{Re}(b)$ is greater or less than one-half. For $\mathrm{Re}(b)$ greater than a half these two boundary conditions reduce to the very simple statement that

$$Q_2\sim Q_3\sim P\epsilon^{\frac{3}{2}b-\frac{3}{4}}. \tag{2.33}$$

In the limit of small bending stiffness, $\epsilon$ tends to zero and $Q_2$ and $Q_3$ are negligible in comparison with $P$. Then the motion upstream of the critical position is given by

$$Y(X)=P\sum_{n=0}^{\infty}\frac{(i\Omega b(X_c-X))^n}{n!\,(n+b-1)!}\quad\text{for }\epsilon\ll X_c-X,\quad \mathrm{Re}(b)>\tfrac{1}{2}. \tag{2.34}$$

When $\mathrm{Re}(b)$ is less than one-half, (2.29) and (2.30) become

$$Q_2\,e^{-i\theta_E}=-Q_3\,e^{i\theta_E}=P\frac{b(-b)!}{(b+1)!}\frac{\Omega^2E^{1+b}}{e^{i\theta_E-i\pi b}-e^{-i\theta_E+i\pi b}}, \tag{2.35}$$

and the cylinder displacement is described by

$$Y(X)=P\left[\sum_{n=0}^{\infty}\frac{(i\Omega b(X_c-X))^n}{n!\,(n+b-1)!}+\frac{\sin\theta_E}{\sin(\theta_E-\pi b)}\frac{b(-b)!}{(b+1)!}\Omega^2E^{1+b}(X_c-X)^{1-b}\right.$$
$$\left.\times\sum_{n=0}^{\infty}\frac{(i\Omega b(X_c-X))^n}{n!\,(n+1-b)!}\right], \tag{2.36}$$

for $\epsilon\ll X_c-X$ and $\mathrm{Re}(b)<\frac{1}{2}$.

We have determined a general expression for the propagation of deflections of frequency $\omega$ along a towed cylinder with a free end in the limit of small bending stiffness. The method of solution involves extending the upstream expression for transverse displacements across a critical point, at which the restoring force due to tension is cancelled by a fluid-loading effect, so that the downstream boundary condition may be applied. The general solution upstream of the critical point is given in (2.34) and (2.36), and is seen to have a different form according to whether $\mathrm{Re}(b)$ is greater or less than one-half. These can be combined into a statement that

$$Y(X)=P\left[\sum_{n=0}^{\infty}\frac{(i\Omega b(X_c-X))^n}{n!\,(n+b-1)!}+H(0.5-\mathrm{Re}(b))\frac{\sin\theta_E}{\sin(\theta_E-\pi b)}\right.$$
$$\left.\times\frac{b(-b)!}{(b+1)!}\Omega^2E^{1+b}(X_c-X)^{1-b}\sum_{n=0}^{\infty}\frac{(i\Omega b(X_c-X))^n}{n!\,(n+1-b)!}\right], \tag{2.37}$$

for $\epsilon \ll X_c - X$ and $\Omega E$ small. An inspection of this expression shows that, when lengths are non-dimensionalized on the cylinder length $l_A$, the displacement at position $X = x/l_A$ depends on the non-dimensional frequency $\Omega = \omega l_A/U$, the ratio $C_N/C_T$ and the value of the parameter $a_A/l_A C_T$. In a particular example the constant $P$ will be determined by the upstream boundary.

Well upstream of the critical position this form for $Y(X)$ simplifies to

$$Y(X) = P \sum_{n=0}^{\infty} \frac{(i\Omega b(X_c - X))^n}{n!\,(n+b-1)!}. \tag{2.38}$$

For $\mathrm{Re}(b)$ greater than a half, this solution is valid throughout the region $X_c - X \gg \epsilon$. But when $\mathrm{Re}(b)$ is less than one-half, it only holds in $X_c - X \gg E$. Then, once $X_c - X$ is comparable in magnitude to $E$, the distance from the critical point to the free end, the second series in (2.37) is important and leads to large gradients of the displacement $Y(X)$. For real frequencies, $\mathrm{Re}(b)$ is equal to $C_N/C_T$. Hence, whenever the normal drag coefficient is less than half the tangential drag coefficient, the displacement of the cylinder has large gradients upstream of the critical position. It is interesting to note that (2.38) describes the motion that would be obtained by applying a boundary condition $i\Omega Y + dY/dX = 0$ at the critical point, i.e. a condition that the cylinder has no normal velocity there. The displacement downstream of the critical position $X_c$ has a more complicated form, and the full expression defined by (2.25*b*) and the boundary conditions (2.29) and (2.30) must be used. The slope of the cylinder is large, but there is little practical interest in the solution in this region.

Ortloff & Ives (1969) expressed their solution to a similar equation in terms of Bessel functions of complex argument and order. $Y(X)$ can be rewritten in a similar form. The series expansion for $J_{b-1}$ shows that

$$\sum_{n=0}^{\infty} \frac{(i\Omega b(X_c - X))^n}{n!\,(n+b-1)!} = (\tfrac{1}{2}\alpha(X_c - X)^{\frac{1}{2}})^{1-b} J_{b-1}(\alpha(X_c - X)^{\frac{1}{2}}). \tag{2.39}$$

where $\alpha = (-4i\Omega b)^{\frac{1}{2}}$, the sign of the square root being chosen so that $\mathrm{Re}(\alpha)$ is positive. Hence, (2.38) is equivalent to

$$Y(X) = P(\tfrac{1}{2}\alpha(X_c - X)^{\frac{1}{2}})^{1-b} J_{b-1}(\alpha(X_c - X)^{\frac{1}{2}}), \tag{2.40}$$

for $0.5 < \mathrm{Re}(b)$ and $X_c - X \gg \epsilon$ or for $0 < \mathrm{Re}(b) < 0.5$ and $X_c - X \gg E$. This form for $Y(X)$ will be found to be convenient when investigating high-frequency disturbances.

## 3. The stability of a towed flexible cylinder

The general solution for the deflections of a towed cylinder derived in §2 may be used to investigate its stability by seeing whether free modes for a fixed upstream end grow or decay in time.

It follows from (2.38) that a condition of no transverse displacement at $X = 0$ is equivalent to

$$\sum_{n=0}^{\infty} \frac{(i\Omega b X_c)^n}{n!\,(n+b-1)!} = 0. \tag{3.1}$$

The complex non-dimensional eigenfrequencies $\Omega$ may be determined from this equation. If one of the roots has negative imaginary $\Omega$, a free mode grows in time and the system is unstable. If, however, all the roots of (3.1) have positive imaginary $\Omega$

the system is stable. It is interesting to note that (3.1) shows that the non-dimensional eigenfrequencies $\Omega$ are determined only by the values of the parameters $C_N/C_T$ and $a_A/l_A C_T$ and are independent of the free-stream velocity $U$. It therefore implies that if the towed cylinder is unstable at any flow speed, it is unstable for all speeds!

We introduce a function $f(\Omega)$ defined by

$$f(\Omega) = (b-1)! \sum_{n=0}^{\infty} \frac{(\mathrm{i}\Omega b X_c)^n}{n!\,(n+b-1)!}, \tag{3.2}$$

$f(\Omega)$ is analytic in the lower half $\Omega$-plane and its number of zeros, $N$, within a closed contour $\Gamma$ in this region is given by Cauchy's theorem as

$$N = \frac{1}{2\pi\mathrm{i}} \oint_{\Gamma} \frac{f'(\Omega)}{f(\Omega)}\,\mathrm{d}\Omega. \tag{3.3}$$

The derivative $f'(\Omega)$ may be evaluated by differentiating (3.2) term by term. The integral (3.3) was evaluated for $C_N/C_T = 0.25$ and $0.75$, $a_A/l_A C_T = 0.033$ and a contour $\Gamma$ consisting of the real $\Omega$-axis from $\Omega = 30$ to $-30$ closed by a semicircle in the lower half $\Omega$-plane. In both cases $N$ was found to be zero, showing that $f(\Omega)$ has no zeros in $\mathrm{Im}(\Omega) < 0$ with $|\Omega|E < 1$. Hence we conclude that for this typical acoustic streamer geometry the towed cylinder is stable for all towing speeds.

## 4. The forced vibration of a towed flexible cylinder

Let us now determine how disturbances produced by vibration of the upstream end of a towed neutrally buoyant cylinder propagate along it. Without loss of generality we will take the amplitude of the transverse vibrations of the upstream end to be unity, and write

$$y(0,t) = \cos\omega t, \tag{4.1}$$

Since $y(x,t) = \mathrm{Re}(Y(X)\,\mathrm{e}^{\mathrm{i}\omega t})$ the boundary condition for $Y(X)$ is

$$Y(0) = 1. \tag{4.2}$$

The coefficient $P$ in the solution (2.38) can be determined from the boundary condition (4.2) to give a form for the displacements of the cylinder:

$$Y(X) = \sum_{n=0}^{\infty} \frac{(\mathrm{i}\Omega b(X_c - X))^n}{n!\,(n+b-1)!} \Big/ \sum_{m=0}^{\infty} \frac{(\mathrm{i}\Omega b X_c)^m}{m!\,(m+b-1)!}. \tag{4.3}$$

For real frequencies, $\mathrm{Re}(b)$ is equal to $C_N/C_T$. Equation (4.3) therefore describes transverse displacements and gradients of the cylinder throughout the region $X_c - X \gg \epsilon$ whenever the normal drag coefficient is greater than half the tangential drag coefficient, but it only holds in $X_c - X \gg E$ when $C_N < \frac{1}{2}C_T$.

The series in (4.3) can be readily evaluated and $Y(X)$ is plotted in figure 4 for $a_A/l_A C_T = 0.033$ and three values of $\Omega$. According to Taylor the ratio $C_N/C_T$ lies between 0 and 1, but we do not know its precise value. Results are therefore presented for two different values of $C_N/C_T$: in figure 4(*a*) $C_N/C_T = 0.25$, while for figure 4(*b*) $C_N/C_T = 0.75$. Lengths have been non-dimensionalized on the cylinder length $l_A$. Before discussing the graphs it is appropriate to investigate the low- and high-frequency limits analytically where simple forms for $Y(X)$ can be derived.

For $\Omega$ sufficiently small, it is enough just to retain the first two terms in the series expansions in (4.3). Then

$$Y(X) \sim 1 - \mathrm{i}\Omega X \quad (\text{for } \Omega \text{ small}), \tag{4.4}$$

i.e. disturbances propagate along the array unchanged in amplitude and with a non-dimensional phase speed of 1. In dimensional terms this means that the phase speed of the disturbance is equal to the flow velocity $U$; the so-called 'worm-in-a-hole' motion. When viewed from a reference frame in which the distant flow field is at rest and the array has a mean speed $U$, the convection and phase speeds are equal and so each element of the array passes through the same physical points. This type of motion has been observed as low-frequency disturbances propagate along a towed array.

The low-frequency asymptotic form described in (4.4) is plotted on figure 4 for comparison with the exact form given in (4.3). There is excellent agreement in the range $\Omega < 1$ (in fact the plots for magnitude overlie).

A simple expression for $Y(X)$ can be derived for high frequencies from the alternative form in (2.40). After applying the boundary condition $Y(0) = 1$ to determine the constant $P$, equation (2.40) shows that (4.3) is equivalent to

$$Y(X) = \left(\frac{X_c - X}{X_c}\right)^{\frac{1}{2}-\frac{1}{2}b} \frac{J_{b-1}(\alpha(X_c - X)^{\frac{1}{2}})}{J_{b-1}(\alpha X_c^{\frac{1}{2}})}. \tag{4.5}$$

For large $|\alpha|(X_c - X)^{\frac{1}{2}}$ and moderate $|b|$, i.e. for $\Omega$ in the range $1 \ll \Omega(X_c - X)$, $\Omega < l_A C_T / a_A$, the large-argument asymptotic form of the Bessel function shows that

$$Y(X) \sim \left(\frac{X_c - X}{X_c}\right)^{\frac{1}{4}-\frac{1}{2}b} \frac{\cos(\alpha(X_c - X)^{\frac{1}{2}} - \frac{1}{2}b\pi + \frac{1}{4}\pi)}{\cos(\alpha X_c^{\frac{1}{2}} - \frac{1}{2}b\pi + \frac{1}{4}\pi)}. \tag{4.6}$$

If $\mathrm{Im}(\alpha)(X_c - X)^{\frac{1}{2}}$ is large, this expression simplifies still further to give

$$Y(X) \sim \left(\frac{X_c - X}{X_c}\right)^{\frac{1}{4}-\frac{1}{2}b} \exp[\mp \mathrm{i}\alpha\{X_c^{\frac{1}{2}} - (X_c - X)^{\frac{1}{2}}\}], \tag{4.7}$$

where the plus sign is appropriate for positive $\mathrm{Im}(\alpha)$, and the minus sign when $\mathrm{Im}(\alpha)$ is negative. Equation (4.7) shows that the amplitude of a high-frequency disturbance decreases rapidly as $X$ increases. The high-frequency asymptotic form described in (4.6) is plotted in figure 4 for $\Omega = 10$, and agrees well with the corresponding exact solution given in (4.3). A comparison of figures 4 (*a*) and 4 (*b*) and the asymptotic form in (4.7) shows that an increase in the normal drag coefficient causes high-frequency disturbances to decrease more rapidly along the array.

We have seen that the form of the forced vibration of a towed cylinder depends on the value of the non-dimensional frequency. At low frequencies disturbances propagate along the cylinder virtually unchanged in amplitude and with a phase speed equal to the towing speed $U$; the so-called 'worm-in-a-hole' motion. At higher frequencies the amplitude of the motion decreases as the disturbances travel downstream along the cylinder.

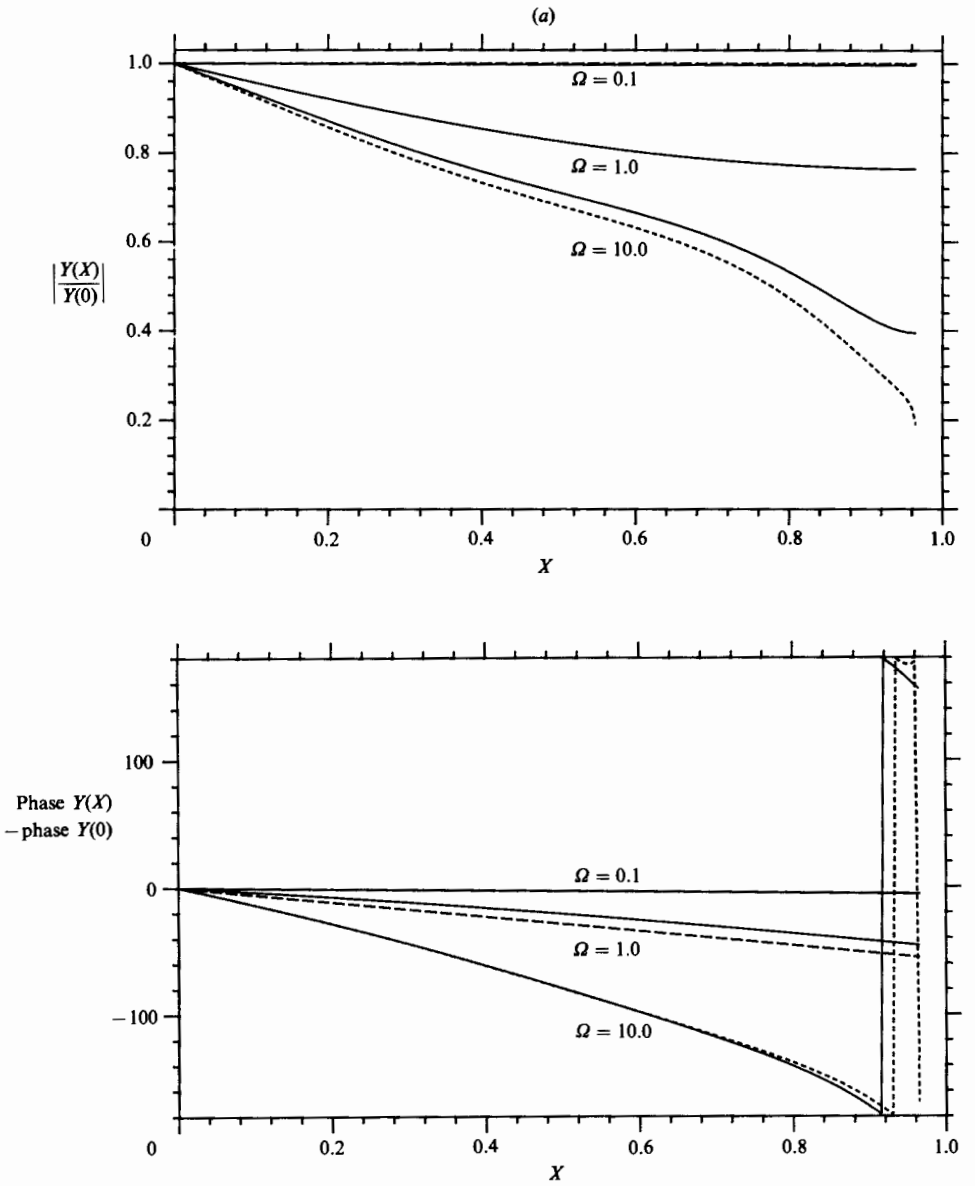


FIGURE 4(*a*). For caption see facing page.

## 5. The effect of a rope drogue

So far the downstream end of the towed cylinder has been considered to be unrestrained, but often there is a rope attached to it acting as a drogue. This arrangement is illustrated in figure 1. In this section the effect of the drogue on the motion of the cylinder is investigated. Let us consider a neutrally buoyant rope drogue with radius $a_{\mathrm{R}}$ and length $l_{\mathrm{R}}$. We will continue to non-dimensionalize lengths on the length $l_{\mathrm{A}}$ of the cylinder, $L = l_{\mathrm{A}}$. Since the rope has a free end, the theory developed in §2 may be used to analyse its motion provided $a_{\mathrm{A}}, l_{\mathrm{A}}$ are replaced by $a_{\mathrm{R}}, l_{\mathrm{R}}$.

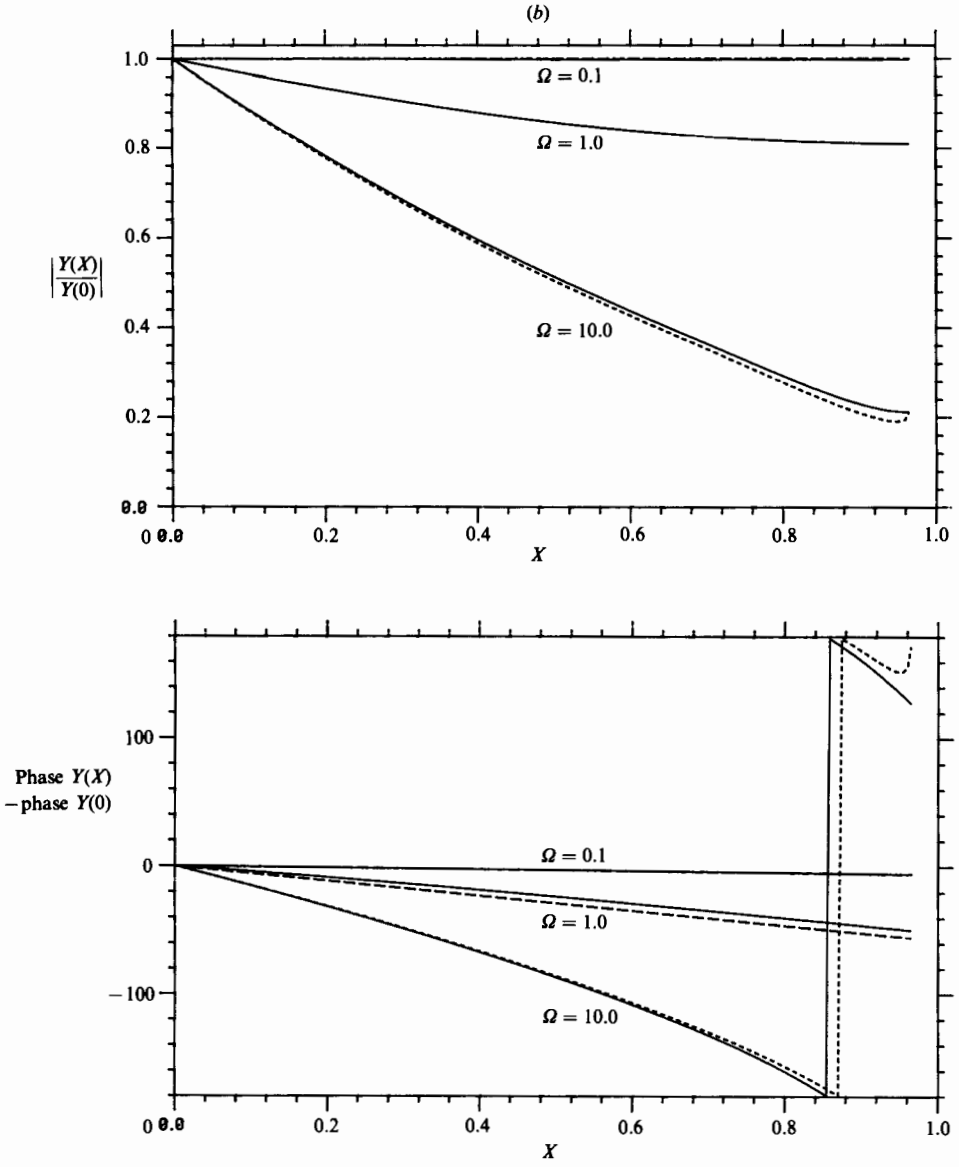


FIGURE 4. Plots of the variation in the magnitude and phase of the transverse displacement with position $X$ along the cylinder for (*a*) $C_N/C_T = 0.25$, (*b*) $C_N/C_T = 0.75$; $a_A/l_A C_T = 0.033$ and three values of $\Omega$. ——, low-frequency asymptotic form (equation (4.4)); - - - - -, high-frequency asymptotic form (equation (4.6)).

The tension at the leading edge of the rope, $T_R$, is given by (2.6);

$$T_R = \rho_0 \pi a_R U^2 C_T l_R. \tag{5.1}$$

This is simply a statement that the tension at the leading edge balances the mean drag on the whole rope. In §2 the form of the solution is significantly affected by the existence of a 'critical point', at which the restoring force due to tension is cancelled by fluid loading. There is a critical point along the rope if

$$T_R > \rho_0 \pi a_R^2 U^2, \tag{5.2}$$

i.e. if $C_T l_R > a_R$. In practice the rope has such a small radius in comparison with its length that this constraint is met. Then the critical point is at a non-dimensional distance $X_{CR}$ downstream of the leading edge of the rope, where from (2.9)

$$l_A X_{CR} = l_R - a_R/C_T. \tag{5.3}$$

Using the full fourth-order differential equation, including bending stiffness, in the region of $X_{CR}$ and applying the boundary condition at the free end will give the general form for transverse displacements of the rope. These are described by (2.37) with $a_A, l_A$ replaced by $a_R, l_R$ and with $L = l_A$. In particular the displacement $Y_R$ and its gradient $dY_R/dX$ at the leading edge of the rope are given by

$$Y_R = R \sum_{n=0}^{\infty} \frac{(i\Omega b_R X_{CR})^n}{n!\,(n+b_R-1)!} + H(0.5-\mathrm{Re}\,(b_R))\, R \frac{\sin\theta_{ER}}{\sin(\theta_{ER}-\pi b_R)} \times \frac{b_R(-b_R)!}{(b_R+1)!}\, \Omega^2 E_R^{1+b_R} X_{CR}^{1-b_R} \sum_{n=0}^{\infty} \frac{(i\Omega b_R X_{CR})^n}{n!\,(n+1-b_R)!}, \tag{5.4}$$

and

$$\frac{dY_R}{dX} = -Ri\Omega b_R \sum_{n=0}^{\infty} \frac{(i\Omega b_R X_{CR})^n}{n!\,(n+b_R)!} - H(0.5-\mathrm{Re}\,(b_R))\, R \frac{\sin\theta_{ER}}{\sin(\theta_{ER}-\pi b_R)} \times \frac{b_R(-b_R)!}{(b_R+1)!}\, \Omega^2 E_R^{1+b_R} X_{CR}^{-b_R} \sum_{n=0}^{\infty} \frac{(i\Omega b_R X_{CR})^n}{n!\,(n-b_R)!}. \tag{5.5}$$

In this expression

$$E_R = a_R/l_A C_T, \tag{5.6}$$

$$\theta_{ER} = \pi(\tfrac{1}{2}b_R - \tfrac{3}{4}) + \tfrac{2}{3}(E_R/\epsilon)^{\frac{3}{2}}, \tag{5.7}$$

$$b_R = \frac{C_N}{C_T} + \frac{2i\Omega a_R}{l_A C_T}, \tag{5.8}$$

and $X_{CR}$ is defined in (5.3). For practical drogues $X_{CR}$ is large in comparison with $E_R$, which is just saying that the critical point on the rope drogue is much closer to its downstream end than to its upstream end. Then the contributions to $Y_R$ and $dY_R/dX$ from the second series in (5.4) and (5.5) are negligible in comparison with that from the first. The constant $R$ is to be determined from boundary conditions at the upstream end of the rope where it joins the cylinder containing the sonar array.

The displacements of the cylinder and rope drogue must be equal at their junction. Also if the join is so short that it has negligible momentum, the forces acting on it must balance. Since the viscous forces acting on a short length are negligible, the balance of the mean longitudinal force reduces to a statement that the tension at the downstream end of the cylinder equals that at the leading edge of the rope. Hence it follows from (5.1) that

$$T(l_A) = T_R = \rho_0 \pi a_R U^2 C_T l_R. \tag{5.9}$$

Substituting this value of $T(l_A)$ into (2.6) gives the tension at a distance $x$ along the cylinder;

$$T(x) = \rho_0 \pi U^2 C_T (a_R l_R + a_A l_A - a_A x). \tag{5.10}$$

An effective drogue is sufficiently long to ensure that

$$l_R a_R C_T > a_A^2, \tag{5.11}$$

so that there is no critical point along the cylinder. Both independent solutions for the transverse motion described in (2.15) and all their derivatives are therefore finite all along the cylinder. When a drogue is long enough to meet the constraint (5.11), the tension it produces in the cylinder is sufficient to eliminate the strong gradients in position that can occur near the free end of an unconstrained cylinder. From (2.15)

$$Y(X) = P \sum_{n=0}^{\infty} \frac{(\mathrm{i}\Omega b_{\mathrm{A}}(X_{\mathrm{CA}}-X))^n}{n!\,(n+b_{\mathrm{A}}-1)!} + Q(X_{\mathrm{CA}}-X)^{1-b_{\mathrm{A}}} \sum_{n=0}^{\infty} \frac{(\mathrm{i}\Omega b_{\mathrm{A}}(X_{\mathrm{CA}}-X))^n}{n!\,(n+1-b_{\mathrm{A}})!}, \quad (5.12)$$

for $0 \leqslant X \leqslant 1$. It follows from (2.13) that

$$b_{\mathrm{A}} = \frac{C_{\mathrm{N}}}{C_{\mathrm{T}}} + \frac{2\mathrm{i}\Omega a_{\mathrm{A}}}{l_{\mathrm{A}} C_{\mathrm{T}}},$$

and substitution for $T(l_{\mathrm{A}})$ from (5.9) into (2.9) shows that

$$X_{\mathrm{CA}} = 1 + \frac{a_{\mathrm{R}} l_{\mathrm{R}}}{a_{\mathrm{A}} l_{\mathrm{A}}} - \frac{a_{\mathrm{A}}}{C_{\mathrm{T}} l_{\mathrm{A}}}. \quad (5.13)$$

The inequality (5.11) ensures that $X_{\mathrm{CA}}$ is greater than unity. The constants $P$ and $Q$ are to be determined from boundary conditions at the two ends of the cylinder $X = 0$ and 1.

Displacements are continuous at the junction of the towed cylinder and the rope i.e.

$$Y(1) = Y_{\mathrm{R}}, \quad (5.14)$$

where $Y(1)$ and $Y_{\mathrm{R}}$ are given by (5.12) and (5.4) respectively.

The second boundary condition at $X = 1$ is that there be no net transverse force acting on the junction of the cylinder and the rope. The only significant forces acting on this joint are those due to the tension in the cylinder and the rope and the virtual mass of the fluid. This virtual-mass term was discussed in the derivation of the free-end boundary condition (2.27). The effects of bending stiffness of the cylinder and any viscous drag on the junction are negligible. The boundary condition is therefore

$$-T(l_{\mathrm{A}})\frac{\partial y_{\mathrm{A}}}{\partial x} + \rho_0 \pi a_{\mathrm{A}}^2 f_{\mathrm{A}} U \left(\frac{\partial y_{\mathrm{A}}}{\partial t} + U\frac{\partial y_{\mathrm{A}}}{\partial x}\right) + T_{\mathrm{R}}\frac{\partial y_{\mathrm{R}}}{\partial x} - \rho_0 \pi a_{\mathrm{R}}^2 f_{\mathrm{R}} U \left(\frac{\partial y_{\mathrm{R}}}{\partial t} + U\frac{\partial y_{\mathrm{R}}}{\partial x}\right) = 0, \quad (5.15)$$

where $y_{\mathrm{A}}$ denotes the displacement at the trailing edge of the towed cylinder and $y_{\mathrm{R}}$ at the leading edge of the rope. The constants $f_{\mathrm{A}}$ and $f_{\mathrm{R}}$ are introduced to account for the three-dimensionality of the flow around the end of the cylinder and rope respectively. The boundary condition (5.15) is similar to that used at the junction of a rope and a cylinder by Hawthorne (1961) and Païdoussis (1968, equation (8)), but they consider a cylinder with considerable bending stiffness and neglect a term due to the tension in the cylinder in their boundary condition. When (5.15) is expressed in terms of non-dimensional variables, for a disturbance with time dependence $\mathrm{e}^{\mathrm{i}\omega t}$, it reduces to

$$Y'(1) - \frac{a_{\mathrm{A}}^2 f_{\mathrm{A}}}{a_{\mathrm{R}} l_{\mathrm{R}} C_{\mathrm{T}}}(\mathrm{i}\Omega Y(1) + Y'(1)) = Y'_{\mathrm{R}} - \frac{a_{\mathrm{R}} f_{\mathrm{R}}}{l_{\mathrm{R}} C_{\mathrm{T}}}(\mathrm{i}\Omega Y_{\mathrm{R}} + Y'_{R}). \quad (5.16)$$

The dash denotes a derivative and $Y'(1)$ can be obtained by differentiating (5.12) term by term. $Y'_{\mathrm{R}}$ is defined in (5.5).

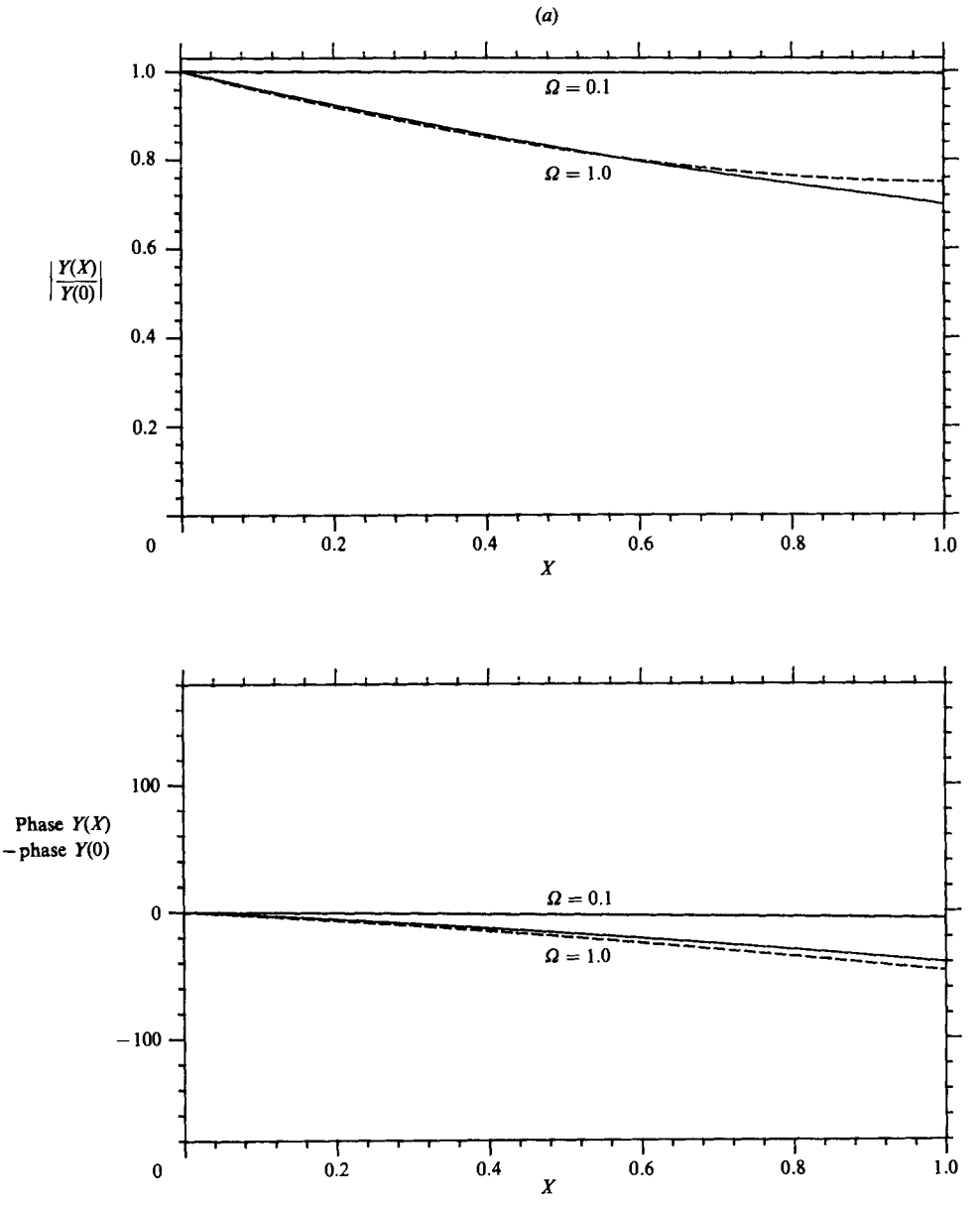


FIGURE 5(*a*). For caption see facing page.

In §3 we found a towed cylinder with a free end to be stable to small transverse displacements. The effect of a rope drogue on the stability can now be investigated. The eigenfrequencies are values of $\Omega$ for which $Y(0) = 0$, where $Y(0)$ is given in (5.12) and $P$ and $Q$ are determined by the boundary conditions (5.14) and (5.16). If there is an eigenfrequency with negative imaginary part, the eigenmode will grow in time and the cylinder and drogue will be unstable. The stability of a cylinder with a drogue has been investigated numerically for $a_A/l_A C_T = 0.033$, $l_R/l_A = 0.15$, $a_R/l_A = 2.4 \times 10^{-5}$, $C_T = 2.5 \times 10^{-3}$ with $f_A = f_R = 1$ and two values of $C_N$; $C_N = 0.25C_T$ and $C_N = 0.75C_T$. The contours Re $Y(0) = 0$ and Im $Y(0) = 0$ were plotted in the lower

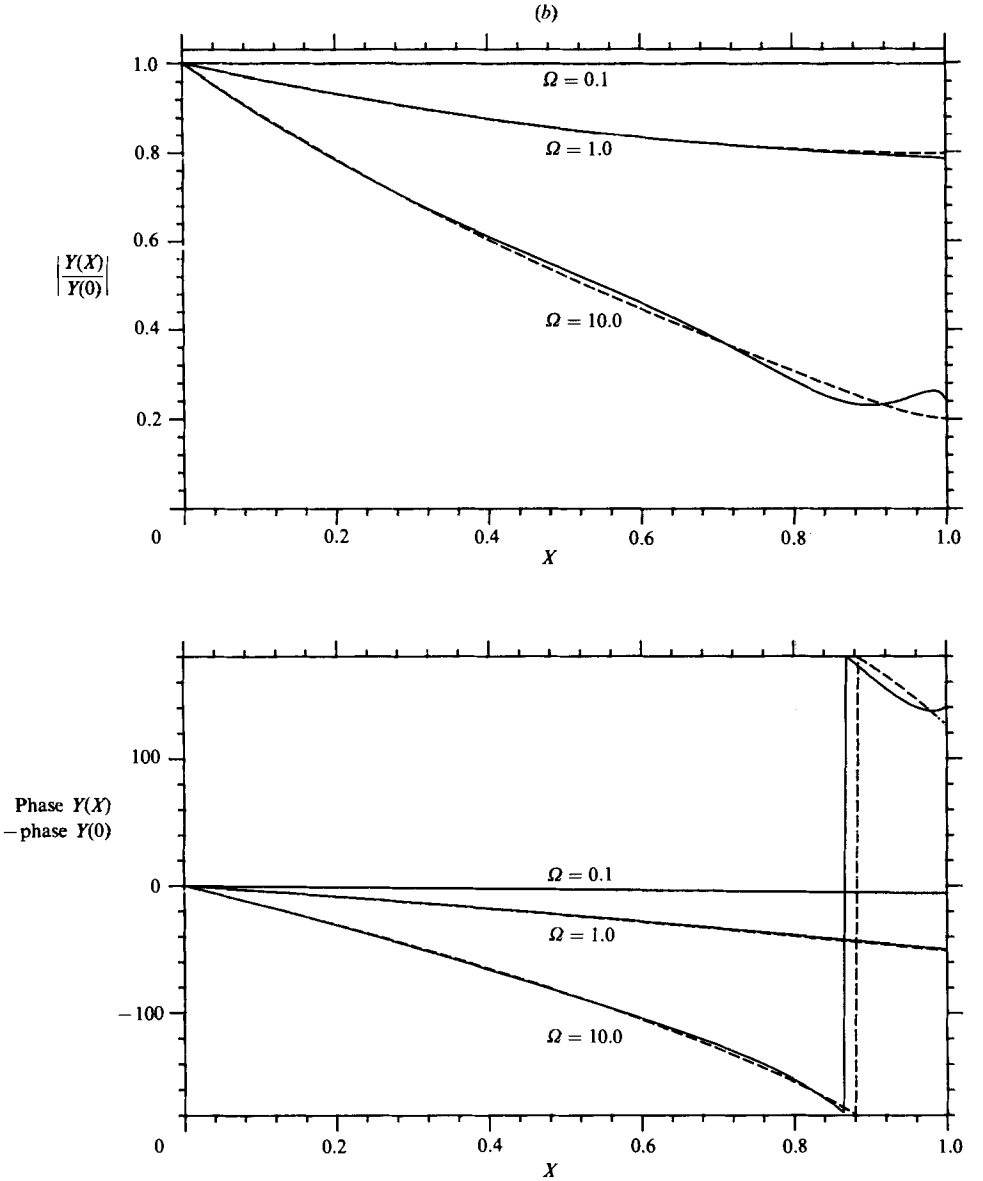


FIGURE 5. Plots of the variation in the magnitude and phase of the transverse displacement with position $X$ along the cylinder for (*a*) $C_N/C_T = 0.25$, (*b*) $C_N/C_T = 0.75$; $a_A/l_A C_T = 0.033$, $l_R/l_A = 0.15$. $a_R/l_A = 2.4 \times 10^{-5}$, $C_T = 2.5 \times 10^{-3}$ with $f_A = f_R = 1$ and different values of $\Omega$. – – –, Magnitude and phase of displacements along a longer cylinder of length $l_A + l_R a_R/a_A$.

half $\Omega$-plane. They were found not to intersect, thereby demonstrating that there are no eigenfrequencies with negative imaginary part. Hence a towed cylinder is not destabilized by the addition of a drogue.

Since the acoustic streamer is stable to towing, it is appropriate to investigate the effect of a drogue on its forced response at frequency $\omega$. Taking the amplitude at the upstream edge of the towed cylinder to be unity gives $y(0, t) = \cos \omega t$ or equivalently

$$Y(0) = 1. \tag{5.17}$$

The coefficients $P$, $Q$ and $R$ can be determined from the three boundary conditions (5.14), (5.16) and (5.17). Once $P$ and $Q$ are known the propagation of disturbances along the cylinder is described by (5.12). This solution is plotted in figure 5 for different frequencies and a cylinder/drogue geometry characterized by $a_A/l_A C_T = 0.033$, $l_R/l_A = 0.15$, $a_R/l_A = 2.4\times10^{-5}$, $C_T = 2.5\times10^{-3}$ with $f_A = f_R = 1$ and two values of $C_N$; $C_N = 0.25C_T$ and $C_N = 0.75C_T$.

When $\Omega(X_{CA}-1)$ is small the effect of the drogue can be investigated analytically. This condition ensures that only the first terms in the series expansions in (5.12) for $Y(1)$ need be retained. Its derivative can be simplified in a similar way. When this approximation is made the boundary conditions (5.14) and (5.16) reduce to a statement that $Q$ is of order $P\Omega(X_{CA}-1)^{b_A}$. Whenever $(\Omega(X_{CA}-1))^{b_A}$ is sufficiently small, the contribution to $Y(X)$ from the second series in (5.12) is negligible in comparison with that from the first i.e.

$$Y(X) \approx P \sum_{n=0}^{\infty} \frac{(i\Omega b_A(X_{CA}-X))^n}{n!(n+b_A-1)!}, \tag{5.18}$$

for $(\Omega(X_{CA}-1))^{b_A} \ll 1$. $P$ can then be determined from the boundary condition (5.17) at the upstream end of the cylinder to give

$$Y(X) = \sum_{n=0}^{\infty} \frac{(i\Omega b_A(X_{CA}-X))^n}{n!(n+b_A-1)!} \Big/ \sum_{m=0}^{\infty} \frac{(i\Omega b_A X_{CA})^m}{m!(m+b_A-1)!}, \tag{5.19}$$

for $(\Omega(X_{CA}-1))^{b_A} \ll 1$. Equation (5.19) is identical in form to (2.38) which describes the motion of a cylinder with a free end. The only difference between these two equations is that $X_c = 1-a_A/l_A C_T$ in (2.38) has been increased to $X_{CA}$ in (5.19). From (5.13)

$$X_{CA} = 1+\frac{a_R l_R}{a_A l_A}-\frac{a_A}{C_T l_A},$$

or in dimensional terms, the critical point is at $l_A+l_R a_R/a_A-a_A/C_T$ for a towed cylinder with a drogue rather than at $l_A-a_A/C_T$. A comparison of these two forms shows that, as far as deflections of most of the cylinder is concerned, a rope drogue has the same effect of increasing the cylinder length by an amount $l_R a_R/a_A$, provided $(\Omega(X_{CA}-1))^{b_A} \ll 1$. The propagation of disturbances along a cylinder of length $l_A+l_R a_R/a_A$ are shown in figure 5 for comparison with the cylinder/drogue results. There is good agreement between the two, confirming the analytical prediction. Kennedy & Strahan (1981) stated that a drogue may have this effect. The constraint that $(\Omega(X_{CA}-1))^{b_A}$ be small is met provided $\Omega l_R a_R/l_A a_A$ is much less than unity. In dimensional variables this is equivalent to $\omega l_R a_R/U a_A \ll 1$.

When $(\Omega(X_{CA}-1))^{b_A}$ is not particularly small, the situation is more complicated and $Q$ may be appreciable. This occurs at high frequencies if $\mathrm{Re}(b_A) = C_N/C_T$ is small. Then the deflection of the cylinder is made up of a superposition of the two linearly independent solutions:

$$Y(X) = PY_1(X)+QY_2(X), \tag{5.20}$$

with

$$Y_1(X) = \sum_{n=0}^{\infty} \frac{(i\Omega b_A(X_{CA}-X))^n}{n!(n+b_A-1)!},$$

and

$$Y_2(X) = (X_{CA}-X)^{1-b_A} \sum_{n=0}^{\infty} \frac{(i\Omega b_A(X_{CA}-X))^n}{n!(n+1-b_A)!}.$$

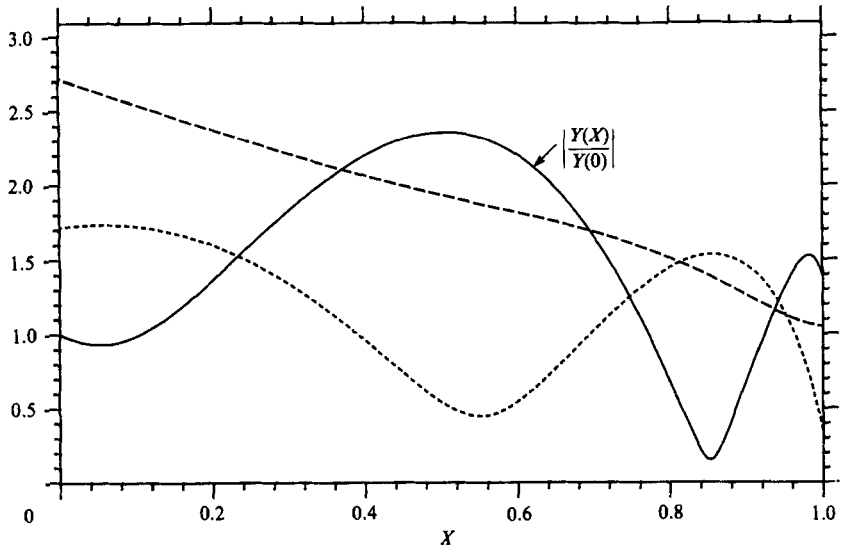


FIGURE 6. Plots of the variation in the magnitude of the transverse displacement with position $X$ along the cylinder for $\Omega = 10$, $C_N/C_T = 0.25$, $a_A/l_A C_T = 0.033$, $l_R/l_A = 0.15$, $a_R/l_A = 2.4 \times 10^{-5}$, $C_T = 2.5 \times 10^{-3}$ with $f_A = f_R = 1$. ---, $|PY_1(X)|$; -----, $|QY_2(X)|$.

An example of this type of behaviour is illustrated in figure 6. A comparison of figures 4(*a*) and 6 shows that in this case the addition of a drogue has had an adverse effect. High-frequency disturbances forced by vibration of the upstream end of the cylinder, decay more slowly with distance along the cylinder with a drogue. The addition of a drogue has admitted a dependence on $Y_2(X)$, which decreases less rapidly than $Y_1(X)$ as $X$ increases.

## 6. Conclusions

The propagation of linear transverse displacements along a neutrally buoyant towed cylinder has been investigated. The form of the deflection is dominated by the existence of a critical point at which the effect of tension in the cylinder is cancelled by a fluid-loading term. Matched asymptotic expansions have been used to extend the solution across the critical point and apply the downstream boundary conditions. Displacements well upstream of the critical point are found to have a simple form, while nearer to the critical point the solution depends on whether the normal drag coefficient $C_N$ is greater or less than half $C_T$.

A typical acoustic streamer geometry has been found to be stable to transverse displacements at all towing speeds. The forced response of the streamer has been investigated so that, in particular, if the time history of the upstream end were known the transverse displacements of the towed cylinder containing a sonar array could be predicted. The motion at a general frequency can be found by summing a series numerically, but for low and high frequencies it has simple analytical forms. Low-frequency disturbances for which $\omega l_A/U \ll 1$ propagate down the array unchanged in amplitude and with a phase speed $U$. This is the so-called 'worm-in-a-hole' motion. Higher-frequency disturbances are more effectively attenuated.

The effect of a rope drogue has been investigated. Provided $\omega l_R a_R/U a_A$ is small in comparison with unity the addition of a drogue has the same effect as increasing

the length of the towed cylinder by $l_R a_R/a_A$. At higher frequencies and for small values of the ratio $C_N/C_T$ attaching a drogue may have an adverse effect, by reducing the attenuation of high-frequency disturbances as they propagate down the cylinder.

I would like to thank Professor J. E. Ffowcs Williams for his illuminating comments during the course of this work. The work has been carried out with the support of Topexpress Ltd and the Procurement Executive, Ministry of Defence.

## Appendix. Asymptotic forms for the inner solution $\Phi_0(R)$

The leading term in the inner expansion is to satisfy (2.19):

$$\frac{\mathrm{d}^4\Phi_0}{\mathrm{d}R^4} - R\frac{\mathrm{d}^2\Phi_0}{\mathrm{d}R^2} - b\frac{\mathrm{d}\Phi_0}{\mathrm{d}R} = 0, \tag{A 1}$$

a third-order differential equation in $\mathrm{d}\Phi_0/\mathrm{d}R$. This may be solved by investigating solutions of the form

$$\frac{\mathrm{d}\Phi_0}{\mathrm{d}R} = \int_0^\infty f(s)\,\mathrm{e}^{s\alpha R}\,\mathrm{d}s, \tag{A 2}$$

where $f(s)$ and $\alpha$ are yet to be determined

Differentiation shows that

$$\frac{\mathrm{d}^4\Phi_0}{\mathrm{d}R^4} = \int_0^\infty s^3\alpha^3 f(s)\,\mathrm{e}^{s\alpha R}\,\mathrm{d}s. \tag{A 3}$$

Similarly

$$R\frac{\mathrm{d}^2\Phi_0}{\mathrm{d}R^2} = \int_0^\infty Rs\alpha f(s)\,\mathrm{e}^{s\alpha R}\,\mathrm{d}s,$$

which after integration by parts becomes

$$R\frac{\mathrm{d}^2\Phi_0}{\mathrm{d}R^2} = -\int_0^\infty \frac{\mathrm{d}}{\mathrm{d}s}(sf(s))\,\mathrm{e}^{s\alpha R}\,\mathrm{d}s, \tag{A 4}$$

provided $sf(s)\mathrm{e}^{s\alpha R}$ tends to zero as $s$ tends both to zero and to infinity. The differential equation (A 1) may therefore be rewritten as

$$\int_0^\infty \left[(s^3\alpha^3 - b)f(s) + \frac{\mathrm{d}}{\mathrm{d}s}\left(sf(s)\right)\right]\mathrm{e}^{s\alpha R}\,\mathrm{d}s \equiv 0 \quad \text{for all } R. \tag{A 5}$$

This is automatically satisfied if the integrand vanishes for all positive $s$, i.e. when $f(s)$ and $\alpha$ are related by

$$\frac{\mathrm{d}f}{\mathrm{d}s} + \left(s^2\alpha^3 + \frac{1-b}{s}\right)f = 0. \tag{A 6}$$

This first-order differential equation for $f$ may be readily integrated to show that, apart from an arbitrary multiplicative constant,

$$f(s) = \mathrm{e}^{-\frac{1}{3}s^3\alpha^3}\,s^{b-1}. \tag{A 7}$$

For $0 < \mathrm{Re}\,(b)$ the condition $sf(s) \to 0$ as $s \to 0$ is met. Finally $\alpha$ is to be chosen to ensure that $sf(s)\,\mathrm{e}^{s\alpha R} \to 0$ as $s \to \infty$. An inspection of (A 7) shows that $\alpha^3 = 1$ will do, i.e.

$$\alpha = 1, \tfrac{1}{2}(-1+\mathrm{i}\sqrt{3}) \quad \text{or } \tfrac{1}{2}(-1-\mathrm{i}\sqrt{3}). \tag{A 8}$$

Substitution for $f(s)$ and $\alpha$ from (A 7) and (A 8) into (A 2) gives three possible solutions of the inner differential equation (A 1):

$$\frac{\mathrm{d}\Phi_0}{\mathrm{d}R} \equiv I_1(R) = \int_0^\infty s^{b-1} \exp\left[-\tfrac{1}{3}s^3 + sR\right] \mathrm{d}s, \tag{A 9a}$$

$$\frac{\mathrm{d}\Phi_0}{\mathrm{d}R} \equiv I_2(R) = \int_0^\infty s^{b-1} \exp\left[-\tfrac{1}{3}s^3 + \tfrac{1}{2}(-1+\mathrm{i}\sqrt{3})\, sR\right] \mathrm{d}s, \tag{A 9b}$$

$$\frac{\mathrm{d}\Phi_0}{\mathrm{d}R} \equiv I_3(R) = \int_0^\infty s^{b-1} \exp\left[-\tfrac{1}{3}s^3 + \tfrac{1}{2}(-1-\mathrm{i}\sqrt{3})\, sR\right] \mathrm{d}s. \tag{A 9c}$$

The asymptotic forms of the integrals $I_1$, $I_2$ and $I_3$ for large $|R|$ will now be evaluated. These are needed to match $\Phi_0(R)$ to the outer solution, but will also show that the three solutions in (A 9) are linearly independent.

$I_1(R)$ is given by

$$I_1(R) \equiv \int_0^\infty s^{b-1} \exp\left[-\tfrac{1}{3}s^3 + sR\right] \mathrm{d}s. \tag{A 10}$$

When $R$ is large and negative, the argument of the exponential is negative throughout the range of integration and the main contribution to the integral comes from near $s = 0$. $I_1$ may be evaluated by Watson's lemma to give

$$I_1(R) \approx (-R)^{-b}\,(b-1)!\,[1+O(R^{-3})] \quad \text{as } R \to -\infty. \tag{A 11}$$

For $R$ large and positive it is appropriate to introduce a new integration variable $p = sR^{-\frac{1}{2}}$

$$I_1(R) \equiv R^{\frac{1}{2}b} \int_0^\infty p^{b-1} \exp\left[R^{\frac{3}{2}}(-\tfrac{1}{3}p^3 + p)\right] \mathrm{d}p. \tag{A 12}$$

The integral now has the form

$$\int_0^\infty g(p) \exp\left[R^{\frac{3}{2}} h(p)\right] \mathrm{d}p,$$

with $h(p) = p - \frac{1}{3}p^3$, and for large $R^{\frac{3}{2}}$ is suitable for evaluation by Laplace's method. It is determined mainly by the region where $h(p)$ is maximum. The maximum of $h(p)$ is at $p = 1$ and $h''(1) = -2$. Laplace's method therefore gives

$$I_1(R) \approx \pi^{\frac{1}{2}} R^{\frac{1}{2}b - \frac{3}{4}} \exp\left[\tfrac{2}{3}R^{\frac{3}{2}}\right] \quad \text{as } R \to +\infty. \tag{A 13}$$

The integral $I_2$ describing the second independent solution can be treated in a similar way

$$I_2(R) \equiv \int_0^\infty s^{b-1} \exp\left[-\tfrac{1}{3}s^3 + \tfrac{1}{2}(-1+\mathrm{i}\sqrt{3})sR\right] \mathrm{d}s. \tag{A 14}$$

When $R$ tends to minus infinity, we introduce a new variable $p = s(-R)^{-\frac{1}{2}}$. In terms of $p$

$$I_2(R) \equiv (-R)^{\frac{1}{2}b} \int_0^\infty p^{b-1} \exp\left[(-R)^{\frac{3}{2}}(-\tfrac{1}{3}p^3 + \mathrm{e}^{-\frac{1}{3}\mathrm{i}\pi} p)\right] \mathrm{d}p. \tag{A 15}$$

The integral is again in the form $\int g(p) \exp\left[(-R)^{\frac{3}{2}} h(p)\right] \mathrm{d}p$, where now $h(p) = -\frac{1}{3}p^3 + \mathrm{e}^{-\frac{1}{3}\mathrm{i}\pi} p$. $h(p)$ has a stationary point at $p = \mathrm{e}^{-\frac{1}{6}\mathrm{i}\pi}$. $\Gamma_1$, the path of steepest descents through this point is sketched in figure 7. As $R \to -\infty$

$$\int_{\Gamma_1} p^{b-1} \exp\left[(-R)^{\frac{3}{2}} h(p)\right] \mathrm{d}p \to \pi^{\frac{1}{2}}(-R)^{-\frac{3}{4}} \exp\left[-\mathrm{i}\tfrac{2}{3}(-R)^{\frac{3}{2}} - \mathrm{i}\pi(\tfrac{1}{6}b - \tfrac{1}{4})\right]. \tag{A 16}$$

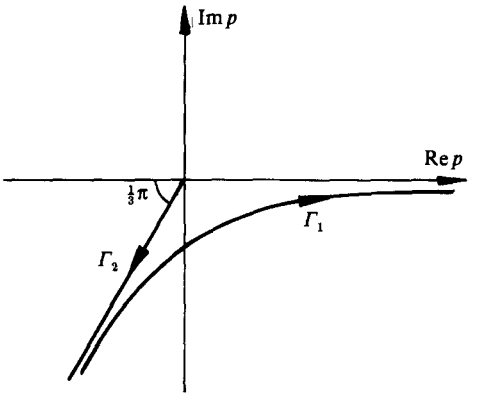


FIGURE 7. The path of steepest descents for the integral in (A 15).

We see from figure 7 that

$$\int_0^\infty p^{b-1}\exp\left[(-R)^{\frac{3}{2}}h(p)\right]\mathrm{d}p = \int_{\Gamma_1+\Gamma_2} p^{b-1}\exp\left[(-R)^{\frac{3}{2}}h(p)\right]\mathrm{d}p, \tag{A 17}$$

where $\Gamma_2$ is the straight line $\arg(p) = -\frac{2}{3}\pi$. $h(p)$ is real on $\Gamma_2$ and becomes increasingly negative as $p$ increases in magnitude along it. Therefore, for large negative $R$, the integral along $\Gamma_2$ may be evaluated by Watson's lemma to give

$$\int_{\Gamma_2} p^{b-1}\exp\left[(-R)^{\frac{3}{2}}h(p)\right]\mathrm{d}p \to (-R)^{-\frac{3}{2}b}\,\mathrm{e}^{-\mathrm{i}\pi\frac{2}{3}b}(b-1)! \quad \text{as } R\to-\infty. \tag{A 18}$$

It then follows from a combination of equations (A 15)–(A 18) that

$$I_2(R) \approx \pi^{\frac{1}{2}}(-R)^{\frac{1}{2}b-\frac{3}{4}}\mathrm{e}^{-\mathrm{i}\pi(\frac{1}{6}b-\frac{1}{4})}\exp\left[-\mathrm{i}\tfrac{2}{3}(-R)^{\frac{3}{2}}\right] + (-R)^{-b}\,\mathrm{e}^{-\mathrm{i}\pi\frac{2}{3}b}(b-1)! \quad \text{as } R\to-\infty. \tag{A 19}$$

When $R$ is large and positive the end-point of integration leads to a larger term than the stationary point. To see this explicitly we make the substitution $p = sR^{-\frac{1}{2}}$ to obtain

$$I_2(R) \equiv R^{\frac{1}{2}b}\int_0^\infty p^{b-1}\exp\left[-R^{\frac{3}{2}}(\tfrac{1}{3}p^3 + \mathrm{e}^{-\frac{1}{3}\mathrm{i}\pi}p)\right]\mathrm{d}p. \tag{A 20}$$

The argument of the exponential is stationary at $p = \mathrm{e}^{\frac{1}{3}\mathrm{i}\pi}$, but the integrand is equal to $\mathrm{e}^{\frac{1}{3}\mathrm{i}\pi(b-1)}\exp\left[-\frac{2}{3}R^{\frac{3}{2}}\right]$ there, and is exponentially small for large $R$. The integral along the real axis can again be expressed as the sum of two integrals, one along the steepest descents curve and the second along a straight line. An appropriate choice of straight line is $p = t\mathrm{e}^{\frac{1}{3}\mathrm{i}\pi}$, with $t$ real $0 \leqslant t \leqslant 1$. The exponential decreases from zero at $t = 0$ along this line, and so for large $R$ the main contribution to the integral comes from near the origin where it can be evaluated by Watson's lemma. This leads to a larger term than the integral along the steepest descents curve through the stationary point and shows that

$$I_2(R) \approx R^{-b}\,\mathrm{e}^{\frac{1}{3}\mathrm{i}\pi b}(b-1)!\left[1+O(R^{-3})\right] \quad \text{as } R\to\infty. \tag{A 21}$$

The asymptotic forms of $I_3(R)$ may be evaluated by a similar method or, more

simply, by noting from (A 9) that the only difference between $I_2(R)$ and $I_3(R)$ is in the sign of i. The complex conjugate of $I_2(R)$ shows

$$I_3(R) = R^{-b}\,\mathrm{e}^{-\frac{1}{3}\mathrm{i}\pi b}\,(b-1)\,![1+O(R^{-3})] \quad \text{as } R\to\infty, \tag{A 22}$$

and

$$I_3(R) \approx \pi^{\frac{1}{2}}(-R)^{\frac{1}{2}b-\frac{3}{4}}\,\mathrm{e}^{\mathrm{i}\pi(\frac{1}{6}b-\frac{1}{4})}\exp[\mathrm{i}\tfrac{2}{3}(-R)^{\frac{3}{2}}]+(-R)^{-b}\,\mathrm{e}^{\frac{1}{3}\mathrm{i}\pi 2b}\,(b-1)! \quad \text{as } R\to-\infty. \tag{A 23}$$

The general solution for $\mathrm{d}\Phi_0/\mathrm{d}R$ may be expressed as a linear combination of the independent solutions $I_1(R)$, $I_2(R)$ and $I_3(R)$;

$$\frac{\mathrm{d}\Phi_0}{\mathrm{d}R} = AI_1(R)+BI_2(R)+CI_3(R), \tag{A 24}$$

where $A$, $B$ and $C$ are arbitrary constants. Integration of the asymptotic forms for $I_1(R)$, $I_2(R)$ and $I_3(R)$ given in equations (A 13), (A 21) and (A 22) shows that for large positive $R$

$$\Phi_0(R) \approx A\pi^{\frac{1}{2}}R^{\frac{1}{2}b-\frac{5}{4}}\exp[\tfrac{2}{3}R^{\frac{3}{2}}]-R^{1-b}\,(b-2)\,!\,(B\,\mathrm{e}^{\frac{1}{3}\mathrm{i}\pi b}+C\,\mathrm{e}^{-\frac{1}{3}\mathrm{i}\pi b})+D, \tag{A 25}$$

where $D$ is a constant arising from the integration. Similarly for large negative $R$ the asymptotic forms in equations (A 11), (A 19) and (A 23) give

$$\Phi_0(R) \approx A(-R)^{1-b}\,(b-2)\,!+(-R)^{1-b}\,(b-2)\,!\,(B\,\mathrm{e}^{-\frac{1}{3}\mathrm{i}\pi 2b}+C\,\mathrm{e}^{\frac{1}{3}\mathrm{i}\pi 2b}) + \pi^{\frac{1}{2}}(-R)^{\frac{1}{2}b-\frac{5}{4}}(B\,\mathrm{e}^{-\mathrm{i}\psi}+C\,\mathrm{e}^{\mathrm{i}\psi})+D, \tag{A 26}$$

with $\psi = \pi(\frac{1}{6}b+\frac{1}{4})+\frac{2}{3}(-R)^{\frac{3}{2}}$.

## REFERENCES


Ablow, C. M. & Schechter, S. 1983 Numerical simulation of undersea cable dynamics. *Ocean Engng* **10**, 443–457.

Hawthorne, W. R. 1961 The early development of the dracone flexible barge. *I Mech. E Proc.* **175**, 52–83.

Huston, R. L. & Kamman, J. W. 1981 A representation of fluid forces in finite segment cable modes. *Computers & Structures* **14**, 281–287.

Ince, E. L. 1956 *Integration of Ordinary Differential Equations.* Edinburgh: Oliver & Boyd.

Ivers, W. D. & Mudie, J. D. 1973 Towing a long cable at slow speeds: a three-dimensional dynamic model. *MTS J.* **7**, 23–31.

Ivers, W. D. & Mudie, J. D. 1975 Simulation studies of the response of a deeply towed vehicle to various towing manoeuvres. *Ocean Engng.* **3**, 37–46.

Kennedy, R. M. 1980 Transverse motion response of a cable-towed system. Part I. Theory. *US J. Underwater Acoust.* **30**, 97–108.

Kennedy, R. M. & Strahan, E. S. 1981 A linear theory of transverse cable dynamics at low frequencies. *NUSC Tech. Rep.* 6463, Naval Underwater Systems Center, Newport, Rhode Island/New London, Connecticut.

Lee, C. 1978 A modelling study on steady-state and transverse dynamic motion of a towed array system. *IEEE J. Oceanic Engng* OE-3, 14–21.

Lee, D. & Kennedy, R. M. 1985 A numerical treatment of a mixed type dynamic motion equation arising from a towed acoustic antenna in the ocean. *Comp. & Maths with Appls.* **11**, 807–816.

Lee, T. S. & D'Appolito, J. A. 1980 Stability analysis of the Ortloff and Ives equation. *TASC Tech. memo.* 1588–1.

LIGHTHILL, M. J. 1960 Note on the swimming of slender fish. *J. Fluid Mech.* **9**, 305–317.

NI, C. C. & HANSEN, R. J. 1978 An experimental study of the flow-induced motions of a flexible cylinder in axial flow. *Trans ASME* I: *J. Fluids Engng* **100**, 389–394.

ORTLOFF, C. R. & IVES, J. 1969 On the dynamic motion of a thin flexible cylinder in a viscous stream. *J. Fluid Mech.* **38**, 713–720.

PAÏDOUSSIS, M. P. 1966 Dynamics of flexible slender cylinders in axial flow: Part 1. Theory. *J. Fluid Mech.* **26**, 717–736.

PAÏDOUSSIS, M. P. 1968 Stability of towed, totally submerged flexible cylinders. *J. Fluid Mech.* **34**, 273–297.

PAÏDOUSSIS, M. P. 1973 Dynamics of cylindrical structures subjected to axial flow. *J. Sound Vib.* **29**, 365–385.

PAÏDOUSSIS, M. P. & YU, B. K. 1976 Elastohydrodynamics of towed slender bodies: the effect of nose and tail shapes on stability. *J. Hydronautics* **10**, 127–134.

PROKHOROVICH, V. A., PROKHOROVICH, P. A. & SMIRNOV, L. V. 1982 Dynamic stability of a flexible rod in a longitudinal incompressible fluid flow. *Sov. Appl. Mech.* **18**, 274–279.

SANDERS, J. V. 1982 A three-dimensional dynamic analysis of a towed system. *Ocean Engng* **9**, 483–499.

TAYLOR, G. I. 1952 Analysis of the swimming of long and narrow animals. *Proc. R. Soc. Lond.* A **214**, 158–183.